ACS OMEGA

http://pubs.acs.org/journal/acsodf

Article

Efficient Separation of Acetylene-Containing Mixtures Using ZIF-8 Membranes

Shiyuan Zhu, Quanjie Lin, Xiaopeng Huang, Liangji Chen, Lizhen Liu, Zizhu Yao,* and Shengchang Xiang*

Cite This: *ACS Omega* 2021, 6, 33018−33023

Read Online

ACCESS | Metrics & More | Article Recommendations | Supporting Information

ABSTRACT: Metal−organic framework (MOF) membranes show great potential in the separation of acetylene mixtures. In this work, we have prepared ZIF-8 membranes on polyamide (PA) substrates for the highly selective separation of acetylene/methane and acetylene/carbon dioxide mixtures. The C_2H_2/CH_4 and C_2H_2/CO_2 mixtures can be successfully separated using the ZIF-8 membranes, with separation factors of 12.1 and 1.8, respectively. Based on the results of the cross-permeation tests of C_2H_2/CH_4, CO_2/CH_4, and C_2H_2/CO_2, the separation mechanism of C_2H_2/CH_4 in our ZIF-8 membrane can be attributed to a higher affinity for acetylene and molecular sieving effect, while C_2H_2/CO_2 separation is related to thermodynamic factors. It is worth noting that this is the first example of MOF membranes to successfully separate C_2H_2 from CH_4 and CO_2.

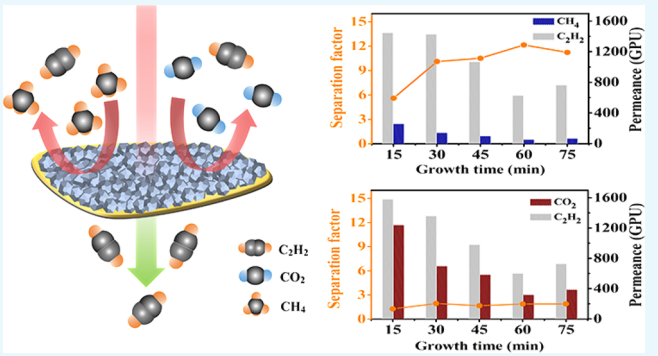

INTRODUCTION

As one of the most important chemical raw materials, acetylene is produced from natural gas by methane coupling at high temperatures[1] so that methane is inevitably mixed in acetylene. The purification of methane-containing acetylene gas in industry relies on the use liquid adsorbents, such as *N*-methylpyrrolidone, in a multistage shower column.[2,3] It is a process that requires complex solvent circulation and additional flash vaporization to desorb the dissolved acetylene, which needs large-scale equipment and increases energy consumption.[4] In addition, owing to the same fluid properties of acetylene and CO_2, the efficient separation of C_2H_2/CO_2 mixtures is another technologically interesting issue. Therefore, a more efficient and rapid purification of acetylene gas is of great importance in optimizing the acetylene production process, increasing production efficiency, and reducing energy consumption and operating costs.

Recently, the emerging microporous metal−organic frameworks (MOFs)-based[5−10] physical adsorbents are promising as cost-effective and efficient materials for C_2H_2 mixture separation. Several MOFs have exhibited high separation capacities and selectivity for C_2H_2/CH_4[11,12] and C_2H_2/CO_2[11,13] through dynamic column breakthrough. However, the regeneration process is inevitable due to the saturated adsorption of the column, in which the configuration and operating costs will increase, furthermore requiring extra energy input.[14] The gas separation membranes raise attention due to the advantages of continuous separation and characteristics without extra input energy for regeneration.[15−17] Although efficient separation of C2 mixtures has been achieved using inorganic molecular sieve membranes,[18] graphene membranes,[19] and polymer membranes,[20] their development have been limited due to the low designability of the materials themselves. MOF-based membranes show powerful designability. Several substrate-supported MOF membranes have been successfully prepared and exhibit high separation performance for binary mixtures with an obvious difference in kinetic diameter. For example, the high-efficiency separation of hydrogen from various mixtures was realized, including H_2/N_2,[21] H_2/CO_2,[22] H_2/CH_4,[23] and H_2/C_3H_8.[24] For some gas mixtures with certain kinetic diameter differences, substrate-supported MOF membranes can also realize effective separation. Sainath et al. grew ZIF-67 crystals on the lumen side of a graphene-modified hollow fiber membrane support using an in situ growth method, and the membranes achieved a CO_2 permeance of 39.25 ± 2.30 GPU (gas permeation unit) with a CO_2/CH_4 selectivity of 44.94 ± 3.0 at 1 bar feed pressure and 25 °C.[25] Alam et al. directly synthesized SAPO-34 membranes on tubular α-alumina supports, and the

Received: September 15, 2021
Accepted: November 10, 2021
Published: November 19, 2021

https://doi.org/10.1021/acsomega.1c05126
ACS Omega 2021, 6, 33018−33023

membranes achieved a N_2 permeance of 399 GPU with a N_2/CH_4 selectivity of 4.38 at 100 kPa and 313 K.[26] Zhou et al. prepared ZIF-8 membranes on porous anodic aluminum oxide supports by a fast current-driven synthesis strategy, and the membranes achieved a C_3H_6 permeance of 52.0 GPU with a C_3H_6/C_3H_8 selectivity of 304.8 at 1 bar and room temperature.[27] However, using MOF membranes to separate gases with similar kinetic diameter is still a challenge, and no MOF membranes have been reported for C_2H_2/CH_4 or C_2H_2/CO_2 separation.

Substrate-supported ZIF-8 membranes have been widely studied because of their simple synthesis. Considering kinetic diameters of 3.3 Å for C_2H_2 and 3.8 Å for CH_4, it is feasible to use the molecular sieving effect of ZIF-8 to achieve C_2H_2/CH_4 separation. For the C_2H_2/CO_2 mixture, the higher affinity for C_2H_2 and ZIF-8 than CO_2 and ZIF-8 is therefore expected to be used for separating these two gases with the same kinetic diameters.[28] In this work, we prepared continuous and dense ZIF-8 membranes through an improved constant-current cathodic deposition method[27,29−33] at room temperature using PA filter membranes as substrates. The separation performance of the ZIF-8 membranes for a series of equimolar binary gas mixtures, including C_2H_2/CH_4, C_2H_2/CO_2, CO_2/CH_4, and C_2H_2/C_2H_4, was tested under atmospheric pressure and room temperature permeation conditions. The results show that our ZIF-8 membranes have a maximum separation factor of 12.1 for the binary C_2H_2/CH_4 gas mixture, corresponding to a permeance of 628.3 GPU for C_2H_2. The ZIF-8 membrane can also separate C_2H_2/CO_2, and the separation factor is 1.8. Cross-permeation tests of C_2H_2/CH_4, CO_2/CH_4, and C_2H_2/CO_2 exhibit both a molecular sieve effect and thermodynamic potential. Preferential permeation induced by ZIF-8's higher affinity for C_2H_2 plays an important role in C_2H_2/CH_4 separation, while the C_2H_2/CO_2 separation is related to thermodynamic factors.

RESULTS AND DISCUSSION

The experimental electrochemical deposition system is shown in Scheme 1. The structure and chemical properties of the prepared ZIF-8 membranes were characterized by powder X-ray diffraction (PXRD) and scanning electron microscopy (SEM). The investigation was conducted at 15 min (ZIF-8 M-15), 30 min (ZIF-8 M-30), 45 min (ZIF-8 M-45), 60 min (ZIF-8 M-60), and 75 min (ZIF-8 M-75). PXRD suggests that both the original PA substrate and the Au-coated PA substrate exhibit diffraction broad peaks typical of polymers (Figure 1). The characteristic diffraction peak of the ZIF-8 membrane at different growth times matched well the simulated ZIF-8 diffraction peak, indicating the successful growth of the ZIF-8 phase on the Au-coated PA substrate. In the top-view SEM images of the membrane (Figure 2), it can be observed that the ZIF-8 upper surface has protruding forms similar to the Au-coated PA substrate at the shorter 15 min growth time since the growth of ZIF-8 is directly related to the electroreduction of ligand dissociated protons[27] and ZIF-8 preferentially grows at locations with higher conductivity.[30] In addition, we note that the size of grains on the membrane surface becomes significantly larger with growth time. This is probably due to the crystallization of Zn^{2+} and ligands in solution, which reduces the concentration of free Zn^{2+} and ligands and then enlarges the grain size. The mother solution changed from clear to turbid with an increase in time, indicating the spontaneous crystallization of the mother solution (Figure S1). The membrane cross-sectional SEM image (Figure 3) shows the increase in thickness of the membrane with growth time. We plot the membrane thickness as a function of growth time. As shown in Figure S2, the membrane thickness increases linearly from 500 to 820 nm, while the growth time increased from 15 to 45 min. While the growth time increased up to 60 and 75 min, the membrane thickness increases slowly to 890

Scheme 1. Schematic Illustration of the Preparation of ZIF-8 on Polyamide Substrates Using Cathodic Deposition[a]

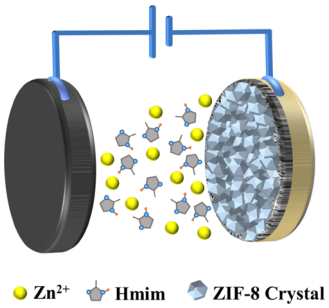

[a]The Au-coated PA substrate serves as a cathode and graphite plates of the same size as anodes in the electrochemcial deposition system.

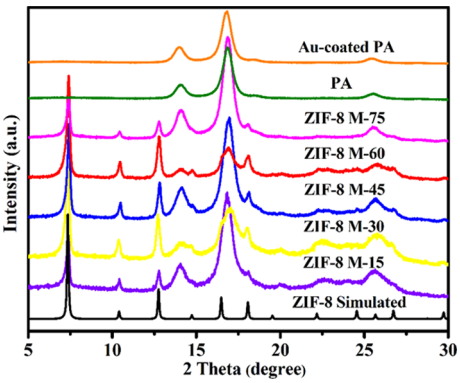

Figure 1. XRD patterns of the PA-supported ZIF-8 membranes at different growth times compared with the PA substrate, the Au-coated PA substrate, or the simulated ZIF-8.

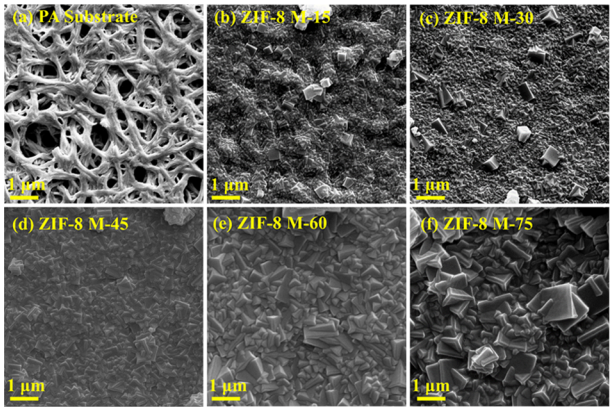

Figure 2. Top-view images of the (a) PA substrate and PA-supported ZIF-8 membranes with different growth times: (b) ZIF-8 M-15, (c) ZIF-8 M-30, (d) ZIF-8 M-45, (e) ZIF-8 M-60, and (f) ZIF-8 M-75.

https://doi.org/10.1021/acsomega.1c05126
ACS Omega 2021, 6, 33018−33023

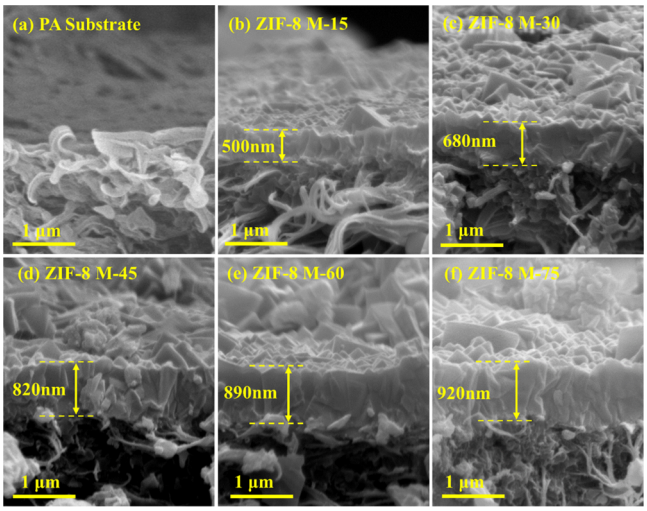

Figure 3. Cross-sectional image of the (a) PA substrate and PA-supported ZIF-8 membranes with different growth times: (b) ZIF-8 M-15, (c) ZIF-8 M-30, (d) ZIF-8 M-45, (e) ZIF-8 M-60, and (f) ZIF-8 M-75.

and 920 nm, respectively, indicating a significant decrease in the rate of the deposition reaction compared to the previous one. The slowing down of the membrane growth rate over time is related to the poor conductivity of ZIF-8, which prevents the substrate to contact the mother liquid directly.[30] In addition, the presence of the ultrathin ZIF-8 layer results in a significant thin-film interference phenomenon on the film surface (Figure S3).

Subsequently, we used the Wicke−Kallenbach-type gas separation measurement system (Figures S4 and S5) to measure the separation of four kinds of equimolar mixtures by ZIF-8 membranes prepared under different growth times. As expected, the separation for C_2H_2/CH_4 mixtures can be efficiently achieved using ZIF-8 membranes. The selectivity factors for C_2H_2/CH_4 increase with the increasing growth time, reaching a maximum of 12.1 at a growth time of 60 min (relevant calculation methods are presented in the Supporting Information). The selectivity factor has a slight decrease of 11.2, while the growth time reaches 75 min, which may be attributed to the further depletion of protons late in the electrodeposition reaction, resulting in excessive concentrations near the cathode, corroding the membrane, leading to membrane defects.[29] The permeances of C_2H_2 and CH_4 show a U-shaped curve with increasing growth time, and both obtained minimum values of 628.3 and 51.9 GPU, respectively, at a growth time of 60 min. Compared to kinetic diameters of C_2H_2 (3.3 Å) and CH_4 (3.8 Å) with a window size of ZIF-8 (3.4 Å), the molecular sieving effect of ZIF-8 works here. We further measure the separation performance of the ZIF-8 membranes for equimolar C_2H_2/CO_2. As shown in Figure 4b, the C_2H_2/CO_2 mixture can also be separated with a selectivity factor of about 1.8, even though the two gases have the same kinetic diameter, indicating that the thermodynamic potential for preferential permeation induced by ZIF-8's higher affinity for C_2H_2 plays an important role in C_2H_2/CO_2 separation. To further confirm this view, we measured the separation performance for CO_2/CH_4 using the ZIF-8 membranes above. As shown in Figure 4c, the change in the selectivity factor is similar to Figure 4a but with an obviously low CO_2/CH_4 separation factor of 6.7 for ZIF-8 M-60, which can be attributed to the lower adsorption enthalpy for CO_2 than C_2H_2. Last, we further test the separation performance of ZIF-8 membranes for equimolar C_2H_2/C_2H_4 (Figure 4d) and also found that ZIF-8 M-60 exhibits the highest selectivity.

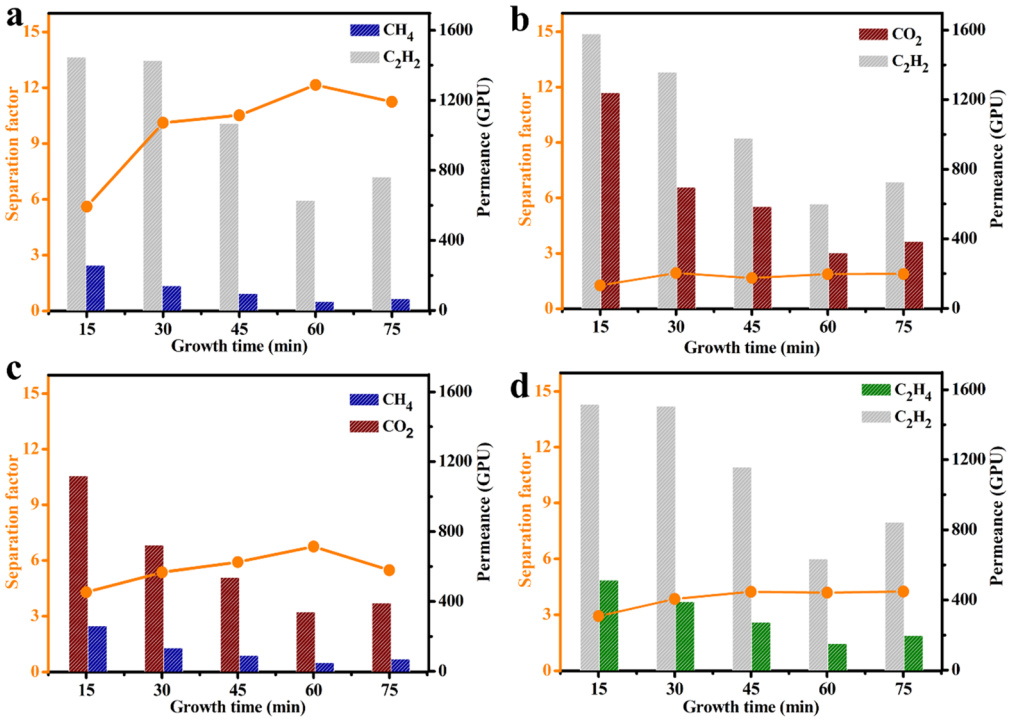

Figure 4. Binary mixture gas separation performance of the PA-supported ZIF-8 membranes with different growth times from 15 to 75 min: (a) C_2H_2/CH_4; (b) C_2H_2/CO_2; (c) CO_2/CH_4; and (d) C_2H_2/C_2H_4.

https://doi.org/10.1021/acsomega.1c05126
ACS Omega 2021, 6, 33018−33023

Table 1. Data Related to Separation for ZIF-8 M-60 Membranes[a]

mixture gas	adsorption enthalpy (kJ/mol)	kinetic diameter (Å)	permeance (GPU)	separation factor	AE diff	KD diff
C_2H_2/CH_4	17.3/12[34]	3.30/3.80	628.3/51.7	12.1	5.3	−0.5
CO_2/CH_4	14.9[35]/12	3.30/3.80	340.4/50.4	6.4	2.9	−0.5
C_2H_2/CO_2	17.3[35]/14.9	3.30/3.30	600.5/319.1	1.8	2.4	0
C_2H_2/C_2H_4	17.3/16.2[36]	3.30/4.16	633.6/151.2	4.2	1.1	−0.86

[a]AE diff: adsorption enthalpy differences. KD diff: kinetic diameter differences. AE diff values and KD diff values are obtained by former molecular' data minus the latter molecular' data.

To further understand the separation behavior in ZIF-8 membranes, ZIF-8 M-60 with the best separation effect in our experiment was selected as an example and we present its related data about gas separation in Table 1. Interestingly, we noticed that the permeances for all gases that we measured have shown only small differences, no matter how the composition of the gas mixture changes, indicating that the interactions between the gases can be almost ignored, and the separation process is dominated by the molecular sieving effect and the interactions between gases and ZIF-8's framework. Thus, the difference of adsorption enthalpy (denoted as AE diff) and kinetic diameter (denoted as KD diff) is introduced. We find that the selectivity factor is positively correlated with the AE diff and KD diff. As shown in Table1, ZIF-8 M-60 has the lowest selectivity factor of 1.8 for C_2H_2/CO_2, corresponding to the low AE diff (2.4 kJ/mol) and KD diff (0 Å). For C_2H_2/C_2H_4, ZIF-8 M-60 shows an incremental selectivity factor of 4.2, which may be due to the relatively high KD diff of −0.86. For C_2H_2/CH_4, the largest separation factor of 12.1 in all the gases that we tested can be observed, which may be benefited from the highest AE diff of 5.3 kJ/mol between C_2H_2 and CH_4 and an obvious kinetic diameter difference of 0.5 Å. Compared to C_2H_2/CH_4, ZIF-8 M-60 only has half the separation factor (6.4) for CO_2/CH_4, even though CO_2 has the same kinetic diameter as C_2H_2 (KD diff = 0). We notice that the AE diff in CO_2/CH_4 is 2.9 kJ/mol, lower than the 5.3 kJ/mol in C_2H_2/CH_4. Thus, we speculate that the AE diff may be responsible for the higher selectivity factor in C_2H_2/CH_4 than CO_2/CH_4. We also provide the related data in Table S1 about the gas separation of other samples, including ZIF-8 M-15, ZIF-8 M-30, ZIF-8 M-45, and ZIF-8 M-75, which show similar results to ZIF-8 M-60. Based on the results above, the high separation factor of ZIF-8 membranes for C_2H_2/CH_4 can be attributed to the molecular sieve effect and thermodynamic potential for preferential permeation induced by ZIF-8's higher affinity for C_2H_2, while the separation for C_2H_2/CO_2 can be attributed to only thermodynamic factors. In addition, the hygrothermal stability of the ZIF-8 M-60 sample was investigated (Figure S6). The results showed that there was no significant degradation in the separation performance of the ZIF-8 M-60 sample for the four kinds of gas mixtures, even though ZIF-8 M-60 was exposed to 95 °C and 90% RH for 4 h. Also, the structure of ZIF-8 was retained after the hygrothermal stability test, which can be confirmed by PXRD (Figure S7). The above results indicated the good hygrothermal stability of the ZIF-8 M-60 sample.

CONCLUSIONS

We have observed continuous and dense ZIF-8 membranes using PA filter membranes as substrates and demonstrated that ZIF-8 membranes can efficiently separate C_2H_2/CH_4 and C_2H_2/CO_2 for the first time. The high affinity of the ZIF-8 framework for C_2H_2 and the small kinetic diameter of C_2H_2 are the reasons for the ability of ZIF-8 to separate C_2H_2 mixtures. It is expected that extensive research endeavors on MOF membranes will facilitate the discoveries of better C_2H_2 separation materials.

EXPERIMENTAL SECTION

Materials. All reagents and solvents were used as received from commercial suppliers without further purification. Polyamide (PA) microporous filter membranes (0.5um) were purchased from Zhejiang Haining Yibo Filter Material Co. A DPS-305BF DC power (0−30 V) was from Guangdong HongShengFeng Co. Aluminum rings with an outer diameter of 50 mm, an inner diameter of 42 mm, and a thickness of 1.5 mm was from Hebei PangShi Aluminum Co. An ISC-150-type ion sputtering instrument was from SuProInstruments. A XK-CTS80Z-type constant temperature and humidity control chamber was used. Any reagents used should be kept dry, and moist reagents that adsorb free water will result in an accelerated rate of crystallization of the mother solution for the synthesis of ZIF-8 membranes.

Preparation of the Mother Solution for the Synthesis of ZIF-8 Membranes. A total of 45 mL of methanol was used to dissolve 0.827 g of zinc acetate anhydrous and another 45 mL of methanol to dissolve 0.738 g of 2-methylimidazole. The two solutions were mixed at room temperature and used for the electrodeposition reaction immediately.

Fabrication of ZIF-8 Membranes by Cathodic Deposition with Constant Current. Sputtering of Au atoms on one side of a 50 mm diameter PA filter membrane was implemented by using an ion sputterer at an absolute pressure of 8 Pa and a power of 10 W for 150 s. The Au-coated PA membrane was then fixed with two aluminum rings and connected to the negative terminal of the DC power supply. A graphite plate of 50 mm diameter and 1 mm thickness is connected to the positive side of the DC power supply and used as the anode. Two electrodes were immersed in the precursor solution, and the distance between the two electrodes was kept at 10 mm. A current of 10 mA was applied to a cathode for a period of time to produce the ZIF-8 layer. The prepared membrane was rinsed several times in methanol and dried in air.

Characterization Methods. X-ray powder diffraction (XRD) patterns were measured with a PANalytical X'pert[3] powder diffractometer at 40 kV and 40 mA. The morphology and thickness of the ZIF-8 film were imaged with a Phenom nano (Thermo Fisher Scientific) field emission scanning electron microscope at 15 kV with a secondary electron signal.

ASSOCIATED CONTENT

Supporting Information

The Supporting Information is available free of charge at https://pubs.acs.org/doi/10.1021/acsomega.1c05126.

https://doi.org/10.1021/acsomega.1c05126
ACS Omega 2021, 6, 33018−33023

Details of the gas separation test method and hygrothermal stability test method; photographs of the mother solution (Figure S1); curves of membrane thickness with growth time (Figure S2); photograph of the ZIF-8 membrane with thin-film interference phenomenon (Figure S3); schematic illustration of the Wicke−Kallenbach-type gas separation measurement system and details of the permeation cell (Figures S4 and S5); gas separation performance and XRD patterns of the ZIF-8 membrane after the hygrothermal stability test (Figures S6 and S7); and data related to separation for ZIF-8 membranes at different growth times (Table S1) (PDF)

Raw data and corresponding calculation methods (XLSX)

AUTHOR INFORMATION

Corresponding Authors

Zizhu Yao − *Fujian Provincial Key Laboratory of Polymer Materials, College of Chemistry and Materials Science, Fujian Normal University, Fuzhou 350007, China;* orcid.org/0000-0002-7860-7633; Email: yaozizhu@fjnu.edu.cn

Shengchang Xiang − *Fujian Provincial Key Laboratory of Polymer Materials, College of Chemistry and Materials Science, Fujian Normal University, Fuzhou 350007, China;* orcid.org/0000-0001-6016-2587; Email: scxiang@fjnu.edu.cn

Authors

Shiyuan Zhu − *Fujian Provincial Key Laboratory of Polymer Materials, College of Chemistry and Materials Science, Fujian Normal University, Fuzhou 350007, China*

Quanjie Lin − *Fujian Provincial Key Laboratory of Polymer Materials, College of Chemistry and Materials Science, Fujian Normal University, Fuzhou 350007, China*

Xiaopeng Huang − *Fujian Provincial Key Laboratory of Polymer Materials, College of Chemistry and Materials Science, Fujian Normal University, Fuzhou 350007, China*

Liangji Chen − *Fujian Provincial Key Laboratory of Polymer Materials, College of Chemistry and Materials Science, Fujian Normal University, Fuzhou 350007, China*

Lizhen Liu − *School of Materials Science and Engineering, Fujian University of Technology, Fujian 350118, China;* orcid.org/0000-0001-5846-309X

Complete contact information is available at: https://pubs.acs.org/10.1021/acsomega.1c05126

Notes

The authors declare no competing financial interest.

ACKNOWLEDGMENTS

This work was financially supported by the National Natural Science Foundation of China (22101050, 21971038, 21975044, 21673039, and 21805039), Fujian Science and Technology Department (2020J01152, 2019H6012, and 2020J05189), and Fujian Education Department Project (JAT190418 and JAT190075).

REFERENCES

(1) He, Y.; Zhou, W.; Krishna, R.; Chen, B. Microporous metal-organic frameworks for storage and separation of small hydrocarbons. *Chem. Commun.* **2012**, *48*, 11813−11831.

(2) Wang, Z.; Zheng, D.; Jin, H. Energy integration of acetylene and power polygeneration by flowrate-exergy diagram. *Appl.Energy* **2009**, *86*, 372−379.

(3) Wang, Z.; Zheng, D.; Jin, H. A novel polygeneration system integrating the acetylene production process and fuel cell. *Int.J.Hydrogen Energy.* **2007**, *32*, 4030−4039.

(4) Wang, X.; Gao, J.; Zhang, J.; Zhang, X.; Guo, R. Theoretical and Experimental Studies on Acetylene Absorption in a Polytetrafluoroethylene Hollow-Fiber Membrane Contactor. *Chem.Eng.Technol.* **2015**, *38*, 215−222.

(5) Zhou, H. C.; Kitagawa, S. Metal-organic frameworks (MOFs). *Chem. Soc. Rev.* **2014**, *43*, 5415−5418.

(6) Du, D. Y.; Qin, J. S.; Li, S. L.; Su, Z. M.; Lan, Y. Q. Recent advances in porous polyoxometalate-based metal-organic framework materials. *Chem. Soc. Rev.* **2014**, *43*, 4615−4632.

(7) Furukawa, H.; Cordova, K. E.; O'Keeffe, M.; Yaghi, O. M. The chemistry and applications of metal-organic frameworks. *Sci.* **2013**, *341*, 974.

(8) Long, J. R.; Yaghi, O. M. The pervasive chemistry of metal-organic frameworks. *Chem. Soc. Rev.* **2009**, *38*, 1213−1214.

(9) Zhu, Q. L.; Xu, Q. Metal-organic framework composites. *Chem. Soc. Rev.* **2014**, *43*, 5468−5512.

(10) Lin, Q.; Ye, Y.; Liu, L.; Yao, Z.; Li, Z.; Wang, L.; Liu, C.; Zhang, Z.; Xiang, S. High proton conductivity in metalloring-cluster based metal-organic nanotubes. *Nano Res.* **2020**, *14*, 387−391.

(11) Mukherjee, S.; Sensharma, D.; Chen, K. J.; Zaworotko, M. J. Crystal engineering of porous coordination networks to enable separation of C2 hydrocarbons. *Chem. Commun.* **2020**, *56*, 10419−10441.

(12) Gu, J.; Sun, X.; Kan, L.; Qiao, J.; Li, G.; Liu, Y. Structural Regulation and Light Hydrocarbon Adsorption/Separation of Three Zirconium-Organic Frameworks Based on Different V-Shaped Ligands. *ACS Appl. Mater. Interfaces* **2021**, *13*, 41680−41687.

(13) Di, Z.; Liu, C.; Pang, J.; Chen, C.; Hu, F.; Yuan, D.; Wu, M.; Hong, M. Cage-Like Porous Materials with Simultaneous High C_2H_2 Storage and Excellent C_2H_2/CO_2 Separation Performance. *Angew. Chem., Int. Ed.* **2021**, *60*, 10828−10832.

(14) Qian, Q.; Asinger, P. A.; Lee, M. J.; Han, G.; Mizrahi Rodriguez, K.; Lin, S.; Benedetti, F. M.; Wu, A. X.; Chi, W. S.; Smith, Z. P. MOF-Based Membranes for Gas Separations. *Chem. Rev.* **2020**, *120*, 8161−8266.

(15) Shi, Y.; Liang, B.; Lin, R.-B.; Zhang, C.; Chen, B. Gas Separation via Hybrid Metal−Organic Framework/Polymer Membranes. *Trends Chem.* **2020**, *2*, 254−269.

(16) Yang, L.; Qian, S.; Wang, X.; Cui, X.; Chen, B.; Xing, H. Energy-efficient separation alternatives: metal-organic frameworks and membranes for hydrocarbon separation. *Chem. Soc. Rev.* **2020**, *49*, 5359−5406.

(17) Ren, Y.; Liang, X.; Dou, H.; Ye, C.; Guo, Z.; Wang, J.; Pan, Y.; Wu, H.; Guiver, M. D.; Jiang, Z. Membrane-Based Olefin/Paraffin Separations. *Adv. Sci.* **2020**, *7*, 2001398.

(18) Min, B.; Korde, A.; Yang, S.; Kim, Y.; Jones, C. W.; Nair, S. Separation of C_2−C_4 hydrocarbons from methane by zeolite MFI hollow fiber membranes fabricated from 2D nanosheets. *AIChE J.* **2020**, *67*, No. e17048.

(19) Xu, Y.; Xu, J.; Yang, C. Separation of diverse alkenes from C_2−C_4 alkanes through nanoporous graphene membranes via local size sieving. *J. Membr. Sci.* **2019**, *584*, 227−235.

(20) Khosravi, A.; Sadeghi, M. Separation performance of poly-(urethane−urea) membranes in the separation of C_2 and C_3 hydrocarbons from methane. *J. Membr. Sci.* **2013**, *434*, 171−183.

(21) Li, W.; Su, P.; Li, Z.; Xu, Z.; Wang, F.; Ou, H.; Zhang, J.; Zhang, G.; Zeng, E. Ultrathin metal-organic framework membrane production by gel-vapour deposition. *Nat. Commun.* **2017**, *8*, 406.

(22) Ma, Y.; Dong, Z.; You, M.; Zhang, Y.; Feng, X.; Ma, X.; Meng, J. Formation of a thin and continuous MOF membrane with 2-D MOF nanosheets as seeds via layer-by-layer growth. *Chem. Commun.* **2019**, *55*, 10146−10149.

(23) Zhu, Y.; Liu, Q.; Caro, J.; Huang, A. Highly hydrogen-permselective zeolitic imidazolate framework ZIF-8 membranes prepared on coarse and macroporous tubes through repeated synthesis. *Sep. Purif. Technol.* **2015**, *146*, 68−74.
(24) Hu, Y.; Wei, J.; Liang, Y.; Zhang, H.; Zhang, X.; Shen, W.; Wang, H. Zeolitic Imidazolate Framework/Graphene Oxide Hybrid Nanosheets as Seeds for the Growth of Ultrathin Molecular Sieving Membranes. *Angew. Chem., Int. Ed.* **2016**, *55*, 2048−2052.
(25) Sainath, K.; Modi, A.; Bellare, J. In-situ growth of zeolitic imidazolate framework-67 nanoparticles on polysulfone/graphene oxide hollow fiber membranes enhance CO_2/CH_4 separation. *J. Membr. Sci.* **2020**, *614*, 118506.
(26) Alam, S. F.; Kim, M.-Z.; Kim, Y. J.; Rehman, A. u.; Devipriyanka, A.; Sharma, P.; Yeo, J.-G.; Lee, J.-S.; Kim, H.; Cho, C.-H. A new seeding method, dry rolling applied to synthesize SAPO-34 zeolite membrane for nitrogen/methane separation. *J. Membr. Sci.* **2020**, *602*, 117825.
(27) Zhou, S.; Wei, Y.; Li, L.; Duan, Y.; Hou, Q.; Zhang, L.; Ding, L. X.; Xue, J.; Wang, H.; Caro, J. Paralyzed membrane: Current-driven synthesis of a metal-organic framework with sharpened propene/propane separation. *Sci. Adv.* **2018**, *4*, No. eaau1393.
(28) Shen, J.; Liu, G.; Huang, K.; Jin, W.; Lee, K. R.; Xu, N. Membranes with fast and selective gas-transport channels of laminar graphene oxide for efficient CO_2 capture. *Angew. Chem., Int. Ed.* **2015**, *54*, 697−697.
(29) Wei, R.; Chi, H. Y.; Li, X.; Lu, D.; Wan, Y.; Yang, C. W.; Lai, Z. Aqueously Cathodic Deposition of ZIF-8 Membranes for Superior Propylene/Propane Separation. *Adv. Funct. Mater.* **2019**, *30*, 1907089.
(30) Zhao, Y.; Wei, Y.; Lyu, L.; Hou, Q.; Caro, J.; Wang, H. Flexible Polypropylene-Supported ZIF-8 Membranes for Highly Efficient Propene/Propane Separation. *J. Am. Chem. Soc.* **2020**, *142*, 20915−20919.
(31) Hou, Q.; Zhou, S.; Wei, Y.; Caro, J.; Wang, H. Balancing the Grain Boundary Structure and the Framework Flexibility through Bimetallic Metal-Organic Framework (MOF) Membranes for Gas Separation. *J. Am. Chem. Soc.* **2020**, *142*, 9582−9586.
(32) Hou, Q.; Wu, Y.; Zhou, S.; Wei, Y.; Caro, J.; Wang, H. Ultra-Tuning of the Aperture Size in Stiffened ZIF-8_Cm Frameworks with Mixed-Linker Strategy for Enhanced CO_2/CH_4 Separation. *Angew. Chem., Int. Ed.* **2019**, *58*, 327−331.
(33) Zhang, X.; Li, Y.; Van Goethem, C.; Wan, K.; Zhang, W.; Luo, J.; Vankelecom, I. F. J.; Fransaer, J. Electrochemically Assisted Interfacial Growth of MOF Membranes. *Matter.* **2019**, *1*, 1285−1292.
(34) García Blanco, A. A.; Vallone, A. F.; Korili, S. A.; Gil, A.; Sapag, K. A comparative study of several microporous materials to store methane by adsorption. *Microporous Mesoporous Mater.* **2016**, *224*, 323−331.
(35) Zhang, J. P.; Zhu, A. X.; Lin, R. B.; Qi, X. L.; Chen, X. M. Pore surface tailored SOD-type metal-organic zeolites. *Adv. Mater.* **2011**, *23*, 1268−1271.
(36) James, J. B.; Wang, J.; Meng, L.; Lin, Y. S. ZIF-8 Membrane Ethylene/Ethane Transport Characteristics in Single and Binary Gas Mixtures. *Ind. Eng. Chem. Res.* **2017**, *56*, 7567−7575.

https://doi.org/10.1021/acsomega.1c05126
ACS Omega 2021, 6, 33018−33023